ISSN: 1687-1006 p
ISSN: 2682-3640 e

The Egyptian International Journal of Engineering Sciences and Technology

https://eijest.journals.ekb.eg/

Vol. 46 (2024) 1–10

DOI: 10.21608/EIJEST.2023.181549.1205

Geometry Impact on Flow Characteristics Inside River Intakes

Muhammad Abdul-Muttalib[a,*], Abd Elhamid Khater[b], Mahmoud Refaiey[c], Ahmed K. Dewedar[d]

[a]*Assistant Professor, Civil Engineering Department, Faculty of Engineering at Shoubra, Benha University, Egypt.*
[b]*Assistant Professor, National Water Research Centre, Egypt.*
[c]*Professor, Civil Engineering Department, Faculty of Engineering at Shobra, Benha University, Egypt.*
[d]*Research Assistant, Hydraulics Research Institute, National Water Research Centre, Egypt.*

A R T I C L E I N F O

Article history:

Received 17 December 2022
Received in revised form 10 June 2023
Accepted 23 August 2023
Available online 23 August 2023

Keywords:

diversion channel
numerical models
open channel
intake
Delft3D-FM

A B S T R A C T

Intake is an open channel that usually has a non-uniform flow along its length. The pattern of the flow in lateral intakes is fully three-dimensional. That is why many studies were carried out on the flow characteristics at the intakes. Velocity and direction change in lateral intakes lead to non-consistency and recirculation of the flow. As the result of these whirlpools, depositions are accumulated inside intakes which consequently decrease intake efficiency. High maintenance cost is regularly paid in order to dredge the sedimentation areas and to guarantee and maintain efficiency. The aims of this study were to get a suitable design of the lateral intakes to improve the flow characteristics at junctions. This study is conducted by using a numerical Software Delft3D-FM which used in predicting flows pattern which validated and employed in a parametric study. The model dimensions were assumed based on a real project data at Nile River in Assiut, Egypt. In this study, four models with sharp edges and different bed levels were presented to investigate flow separation zones at different angles of the intake entrance. In order to control the model accuracy in predicting the dimensions of the separated areas, the results were compared with the base configuration which has a flat horizontal bed level of intake. Comparisons between the predicted and the initial configuration velocities at the considered sections indicate that the model captures most of the trends with sensible accuracy. It is concluded that configuration number 4 which has two-fold baffle walls located on the right side has a significant effect on improving flow velocity, circulation zone length, reverse flow width as it enforces the flow to the inner side achieving a good flow distribution inside the intake. The results indicate also that the optimal angle of lateral intake which gives minimum length and width of separation zone is at $\theta = 30^{\circ}$.

1. Introduction

Rivers are considered as one of the providers of pure water for the nature and humans. Rivers have always been one of the most cost-effective ways to convey cooling water to power plants (Raudkivi, 1993) [1]. River flows at main channels and diversions are geometrically similar and belong to the same class of gravity-driven flows that are divided into two directions and two flow ratios. There are different kinds of river diversions that depend on river condition and quantity of water diverted. Lateral intake is one of these diversions where the flows are turbulent (Hamid, 2008) [2]. The construction of these intakes affects the flow characteristics in the junction region, (Yonesi et al., 2008) [3]. In recent

* Corresponding author. Tel.: +0-101-620-8039.
E-mail address: mohamed.ibrahim01@feng.bu.edu.eg.

decades, extensive theoretical and experimental investigations of the junctions have been studied to improve the flow pattern inside lateral intake, (Sayed, 2019) [4].

As the flows enter the turnout it is exposed to separation. This zone of separation is considered a suitable place for the deposition and accumulation of sediments (Barkdoll et al., 1999) [5]. These depositions may cause erosion and destruction of lateral intake cross section, (Shamloo & Pirzadah, 2007) [6]. In addition, some studies show that many pump stations and turnout structures have faced side erosion and many of them have sedimentation problems due to return flow and vortex, (Jalili et al., 2011) [7]. So that, it is important to investigate the pattern of the flow in the separation area to provide solutions to avoid these problems.

2. Flow Separation

At the junctions, the flow is separated into two parts, one moving towards the intake and another flowing in the downstream path along the main channel (Neary et al., 1999) [8].

In 2007, Ramamurthy et al., [9], composed experimentally and numerically a 3D velocity distribution in the junction region at angle 90°. They found that the maximum velocity component occurred near the surface at the entrance of branch channel at the contracted flow. However, this velocity started from negative values in the beginning of the branch channel and reversing the diverted flow to positive values towards the downstream wall. These low values and the recirculation of water in the same place indicated the vortices in this region. They indicated also that the width and length of separation zone in the branching channel decrease with the increasing of discharge ratio Qr (the ratio of the intake discharge to the main discharge). This result agreed with many other studies such as Jalili et al. (2011) [7], Rady (2015) [10], Nikbin and Borghei (2011) [11], Goudarzizadeh et al. (2010) [12], and Seyedian et al. (2008) [13].

3. Intake Geometric Attributes

Both geometry and inclination of lateral intake are very significant to minimize the separation zone at the mouth of the intake. The location and size of this zone depends also on the discharge ratio between the intake and the main channel as mentioned in the previous section. Keshavarzi, & Habibi (2005), [14], studied experimentally five intake angles with 45°, 56°, 67°, 79° and 90°. The separation zone size inside the intake was measured from the plotted streamlines and compared. They showed that the right-angle of the intake produces a large separation zone. They concluded also, from statistical analysis, that a minimum separation size formed in a 55° angle of water intake.

Karami & Keshavarzi (2007), [15], and Ouyang et al. (2009), [16], conducted coupled numerical and physical experiments to investigate flow characteristics in intakes with various lateral intake angles. They showed that the angles between 33° and 55° degrees caused a reduction in the flow separation size.

Rooniyan F., (2014), [17], studied the effect of confluence angle on flow features at a rectangular open channel. In his study, intake angles of 30°, 45° & 60° are used in a numerical model to scrutinize the effect of geometry of the channel junction on both flow pattern and flow separation zone with different discharge ratios. Analysis showed also that the least area of the separation zone will be at an angle of 45°.

Al-Zubaidy & Hilo (2021), [18], used CFD software ANSYS fluent to simulate flow patterns at diversion channel using a variety of geometry designs. These designs included changing the intake's angle and chamfering or rounding the inner corner of the intake entrance instead of the sharp edge. The findings demonstrated that the angle of 30° to 45° is the best configuration for lowering both separation zone dimensions and sediment concentration.

Al Omari and Khaleel (2012), [19], found that the discharge ratio (Qr) is directly proportional with the diverted channel bed slope. Furthermore, the maximum Qr increased by 12.13% when the intake bed slope was transformed from 0.001 to 0.0025 when other variables are fixed.

From previous, the review of the literature showed that most of the studies dealt with lateral intake angle to reduce the separation zone area. Accordingly, this study is concerned to investigate, besides, the lateral intake angle, the effect of different design geometric attributes of river intakes to reduce the circulation and enhance consistency of the flow.

4. Examined Design Attributes

Three parameters were applied as performance indicators to scrutinize improvement in flow separation. These parameters considered flow velocity, circulation zone length, reverse flow width.

The layout of the river intake system showing the parameters listed above are shown in Figure 1. The circulation length and width are considered as Lv, and Wv, respectively, while the intake channel length and width are labeled as Lch and Wch, respectively. Also, the intake channel angle of alignment was labeled as θ.

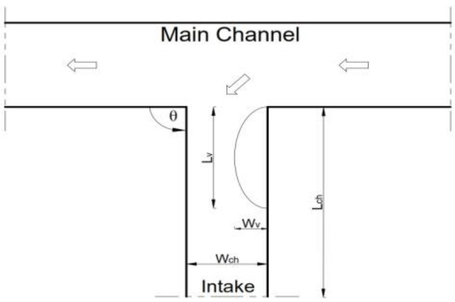

Fig.1: Intake layout with labelling of examined variables including flow separation length Lv, flow circulation width Wv, intake width Wch, intake length Lch and intake angle of alignment Ɵ.

5. Model Design

In this research, lateral intakes will be studied to investigate their effect on the hydrodynamic changes of the flow pattern. These changes are gradients of the transverse pressure in the vicinity of the intake which induce region of different gradients of mean-velocity, depth-varying surface of flow separation, vortices, and zone of flow reversal. In order to assess this phenomenon, a numerical model (Delft-3D FM) was used to test two main design attributes: (i) Intake bed configurations, (ii) Intake horizontal angle (θ) of alignment. For the first design attribute under this study, five bed configurations were examined and will be described in detail afterwards. For the second design attribute, three intake angles (30°, 45°, 60°) were examined in addition to right angle intake for best configuration selected from the bed configuration scenario in terms of minimizing flow vortices.

All dimensions were set in metric system. Five bed configurations were tested in this study to investigate their effect on achieving flow consistency and minimizing vortices. These data in addition to dimensions of the model were assumed based on a real project data at Nile River in Assiut, Egypt. Initial configuration was conducted to be as default configuration with constant bed level (+10.00) m and constant water level (+13.00) to provide water depth of 3 m for comparison with the other four configurations:

a) Five equal steps of 0.4 m each, starting from a bed level of +10.00 m to the end of intake level at +8.00 m as shown in Figure 2-a. Based on this configuration, the step is 40 m long.

b) Unidirectional sloping bed decreasing from +10.00 m to +8.00 m as shown in Figure 2-b.

c) Double sloped bed split along the diagonal of the intake channel as shown in Figure 2-c.

d) Two-fold baffle walls located on the right side with respect to the general flow direction. The first one is located at the entrance with a crest level of +12.00 m and the one after is 40 m in the downstream direction, with a crest level of +11.00 m. The baffle wall is 20 m wide in the crossflow direction and 1 m thick as shown in Figure 2-d.

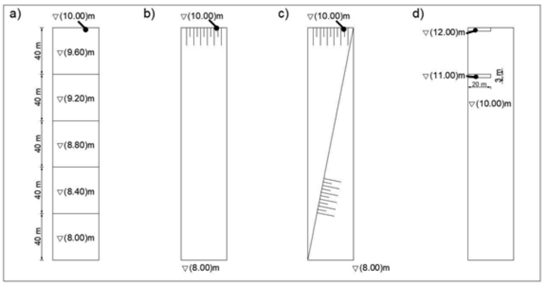

Fig. 2: Intake bed levels of configurations

6. Methodology

6.1 Delft3D-FM Model

Delft3D-FM modeling system is designed to simulate hydrodynamics, morphological, sediment transport, and currents developments, and water quality aspects in rivers (Roelvink and Van Banning, 1994) [20]. All simulations were conducted using Delft-3D FM software. Delft-3D FM model is a process- based model that includes flow, current, and bed evolution modeling which are linked to and integrated with one-another (Hu et al., 2009) [21]. A comprehensive knowledge of Delft-3D FM model is necessary to obtain a reliable result for the hydrodynamic prediction in the area of interest. Delft-3D FM is shown to perform well in several theoretical, laboratory, and real-life situations (Lesser, 2004), [22].

6.2 Model Setup and Grid Design

Realistic discharges and corresponding water levels were imposed into the model. The previous studies at this area showed that the maximum flow conditions have higher water levels and velocities in the main channel compared with minimum flow conditions. Whilst the abstraction quantity of the water intake is fixed over the year. Therefore, in case of maximum flow conditions, the discharge ratio between lateral intake and main channel is lower than its ratio in case of minimum flow conditions. This lowered ratio provided, as mentioned before while describing the formation of separation zone, a larger area of vortices. So that, the considered worst or critical case of flow recirculation inside the intakes appears during the maximum flow conditions. Hence, these maximum conditions were used in this study. All boundary conditions including discharge and water level were kept constant in all configurations to focus on the study objectives, the following approach of model execution is followed:

The water level boundary condition for the model was assumed (+13.00 m). One-month simulation period was assumed with 50-sec time step. For grid structure, it should be fine enough especially near the area of interest and at wall boundaries and junction because there is rapid variation in this region. The size of the grid was selected in a way to make a balance between the accuracy of the grid to represent the details of the junction zone as well as satisfying the required stability of the model solution taking into consideration computational time's consumption (Ammar, 2017) [23]. Various trials were carried out with different number of grids in x and y directions. It was found that results are independent of grid size, if at least 16350 nodes were used. For accuracy reasons, the total number of grid cells is 35325 with 285×120 cells in the main channel and 125×25 cells in the intake. The bathymetric was converted to geometry points and interpolated over the constructed grid. An unstructured grid was used, as shown in Figure 3 with a relative low resolution of 1.6 m cross-line and long-line.

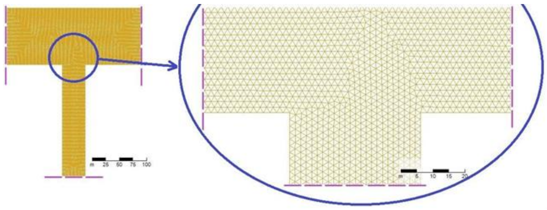

Fig. 3: Grid geometry of model.

The model consisted of two parts, the first part is the main channel which was simulated as a main open channel of river with 900 m length, 100 m width with a constant bed level of (10.00) m, the second part is the lateral intake channel which is located at the center of the model with 200 m length and 40 m width and ends with a sump for flow abstraction. Three boundary conditions were defined: inlet discharge at the right with a constant value of 225 m^3/s and water level at the left boundary with a level of (13.00) m, sump discharge with a value of -

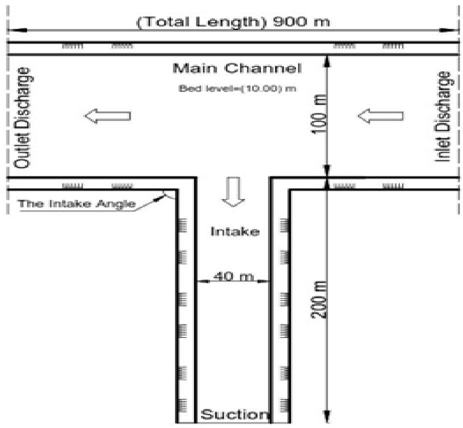

50 m^3/s. Figure 4 shows general model layout of the study describing dimensions and boundaries used.

Fig. 4: Model Layout of the study.

7. Results

Improvements in flow velocities, circulation zone coverage, and reverse flow width ratio were obtained for the four tested configurations. They were simulated based on constant discharge value, water level, bathymetry, and boundary conditions. Comparison was then conducted for the best configuration at the three intake angles (30°, 45°, 60°) in addition to right angle intake.

7.1 Influence of the tested configurations on flow consistency inside intake

Tested parameters were compared to initial configuration as shown in Figure 5 and Figures 6-10. Generally, velocity distribution and consistency improved slightly compared to initial configuration at configurations 1, 2 and 3 and considerably at configuration 4. Specifically, Configuration 1 decreased the flow velocities at the outer curve by 11% compared to initial configuration and minimized the circulation zone by about 8% and the reverse flow width by about 6%. Configuration 2 as configuration 1 decreased the flow velocities by about 17%, the circulation zone by 13 % and the reverse flow width by 12%. Configuration 3 showed better improvement compared to configuration 1 and 2, the flow velocities decreased by 21% and the circulation zone by about 29% and the reverse flow width by 37%. Configuration 4 considerably decreased the flow velocities by 25% and the circulation zone by 54% and reverse flow width by 53%.

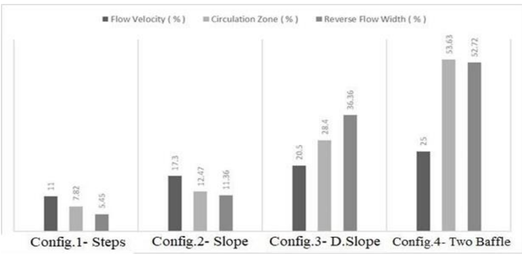

Fig. 5: Improvements in flow velocity, circulation zone and reverse flow width compared to initial configuration for the four configurations.

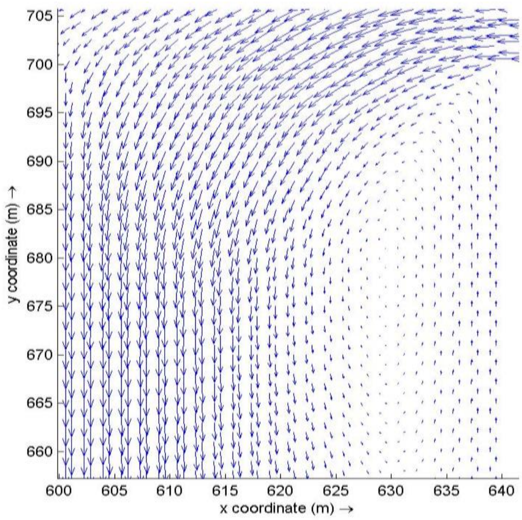

Fig. 6: General result of flow velocities as vectors of Base configuration.

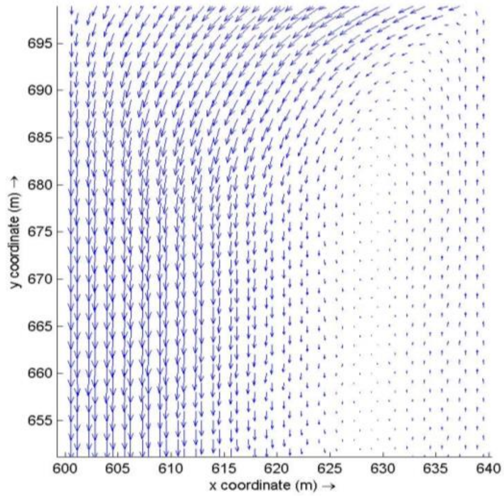

Fig. 7: General result of flow velocities as vectors of configuration (1).

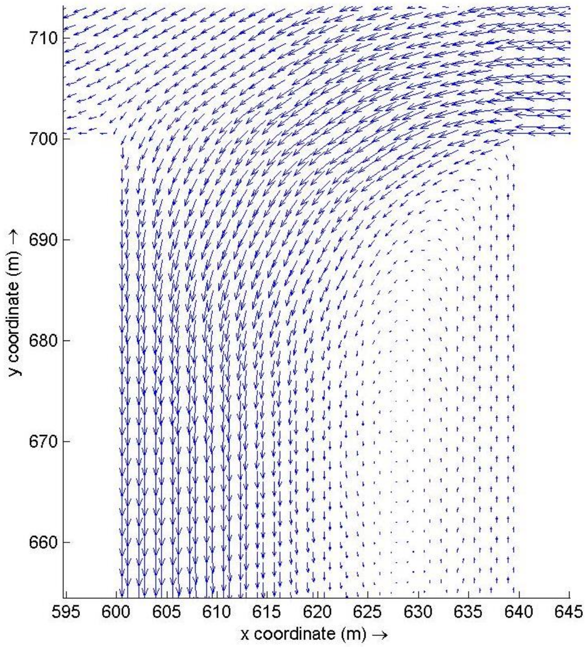

Fig.8: General result of flow velocities as vectors of configuration (2).

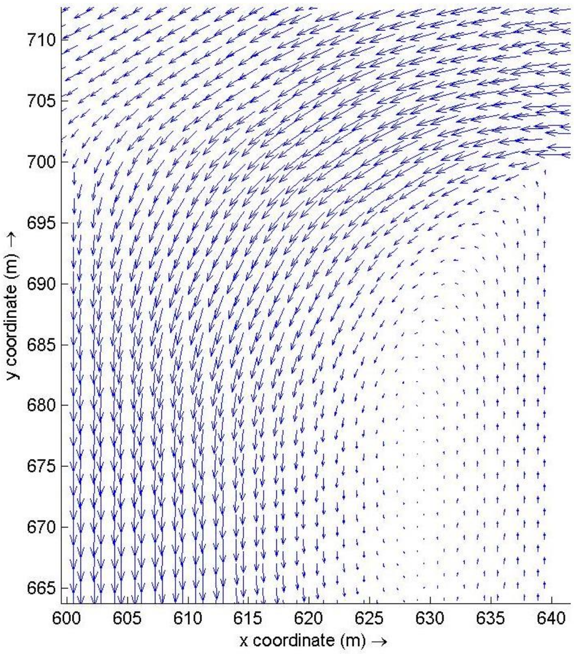

Fig.9: General result of flow velocities as vectors of configuration (3).

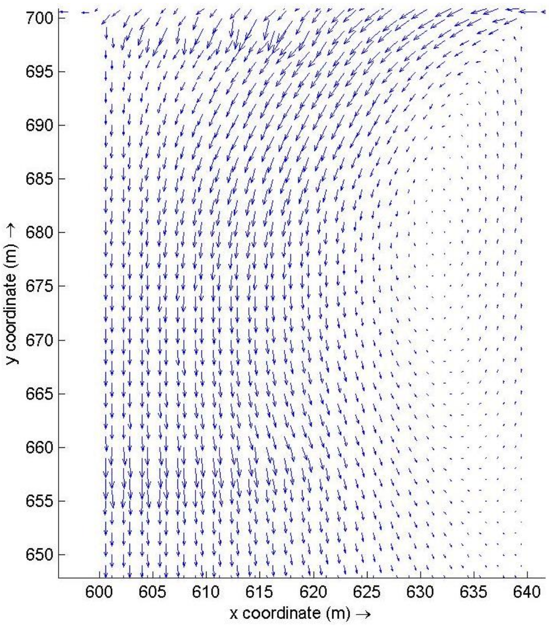

Fig.10: General result of flow velocities as vectors of configuration (4).

To get more detailed results, ten cross sections as shown in Figure 11 were investigated to cover this research phenomena. The most representative changes were observed in cross sections 5, 6, and 7 while the rest showed minor changes. Therefore, cross sections 5, 6 and 7 were chosen to get more detailed insights on the flow consistency for the four tested configurations as well as different studied angles. Each of velocity cross section was compared to initial configuration. The comparison was performed for the depth average velocity which measured from the left side of the intake channel.

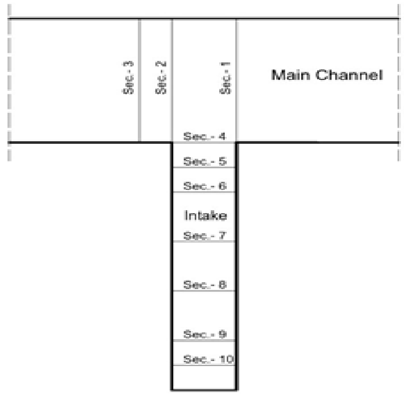

Fig. 11: location of velocity cross sections used for comparison for the four tested configurations.

Figure 12 shows velocity distribution for the four tested configurations compared to initial configuration at cross section 5. Initial configuration showed a reverse flow at left with a negative velocity up to - 0.2 m/s and high velocities at the right that reached 0.9 m/s. The four tested configurations succeeded in minimizing the negative velocities at the left. However, there still negative velocities were appeared. At the right side, configuration 1 decreased the velocity by about 7% and configuration 2 and 3 decreased the velocity by about 18% and showed nearly the same improvements along the whole cross section width. Configuration 4 showed the best improvement and achieved a uniform distribution of velocities which extended from the right to the middle of the cross section.

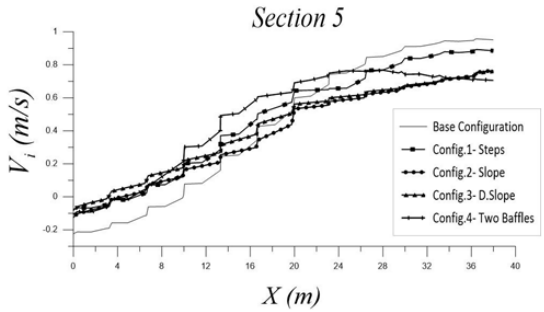

Fig. 12: Velocity distribution for the four tested configurations compared to initial configuration at cross section 5.

At cross section 6, as shown in Figure 13, the velocity distribution of the four tested configurations was plotted against initial configuration. The base case showed a reverse flow at left with a negative velocity up to - 0.2 m/s and high velocities at the right that reached 0.9 m/s. This distribution was improved at configurations 1, 2, 3, and 4 consequently. Negative flow at left side was minimized for configurations 1, 2, and 3 but it was adjusted to positive in case of configuration 4. Therefore, the variation between high velocities at right side and low velocities at left side for configuration 4 was varied from 0.6 m/s to 0.1 m/s however to was varied from 0.9 m/s to - 0.15 m/s for configuration 1. This indicates the positive effect of configuration 4 on improving the consistency of the flow by minimizing the variation between the high and low velocities almost to the half.

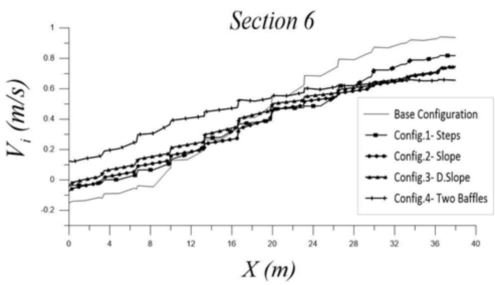

Fig. 13: Velocity distribution for configurations compared to initial configuration at cross section 6.

At section 7, as shown in Figure 14, the reverse flow decreased at the right side but it increased at the left side and became more uniformly distributed. This indicates the effectiveness of the tested configurations. As the variation between high velocities at right side and low velocities at left side for configuration 1, 2, and 3 was changed from 0.6 m/s to 0.1 m/s. While for configuration 4, it was varied from 0.5 m/s to 0.3 m/s if compared to the variation from 0.9 m/s to 0.05 m/s in case of configuration 1. Finally, configuration 4 achieved a semi-uniform flow with no-reverse flow at the left side or higher velocities at the right side.

Velocity distribution was enhanced a little bit for configuration 1, 2 and 3 and remarkably for configuration 4. Hence, configuration 4 was examined for an additional three intake angles (30, 45, and 60 Degrees) to be compared to the right-angle intake at same sections studied earlier 5, 6 and 7.

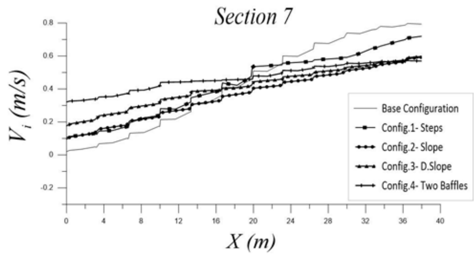

Fig. 14: Velocity distribution for all configurations compared to initial configuration at cross section 7.

7.2 Influence of the tested configurations on flow characteristics in front of the intake

To set a clear view about the influence of geometry on the flow characteristics in the main channel in front of the river side intake, the velocity distribution for different configurations is presented in Figure 15 and Figure 16 for both sections 1 and 3, respectively. In Figure 10, a comparison of all configurations was conducted across the main channel at the upstream corner of the intake. Configurations 1, 2, 3, and the base configuration exhibit a consistent trend in velocity distribution starting with velocity less than the normal depth average velocity by approximately 20 %. But in case of configuration 4, the trend of the velocity distribution is matched with other configurations along the main channel width, except for the first 10 % of its width, it shows a slight increase by 3 % in average than other configurations. Besides, for all configurations the velocities are stabilized after traversing almost 50 % of the main channel width.

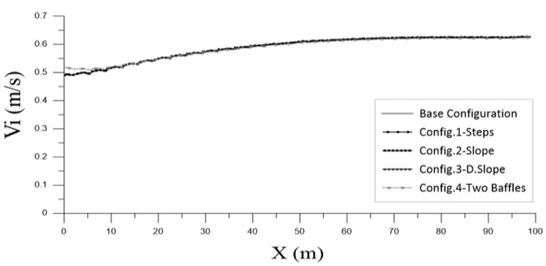

Fig. 15: Velocity distribution for all configurations compared to initial configuration at cross section 1.

In Figure 16, a comparison of all configurations was carried out across the main channel at the downstream corner of the intake. The velocities distributions for configurations 1, 2, 3, and the base configuration are in a good match. These distributions start with a velocity higher than the normal depth average velocity by approximately 18

%. Moreover, in the case of configuration 4, the velocity distribution is consistent also with other configurations along the main channel width, except for the first 12 % of its width, it demonstrates a slight increase of velocity by 5 % in average than other configurations. Similarly, to Figure 10, for all configurations the velocities are stabilized after traversing almost 50 % of the main channel width.

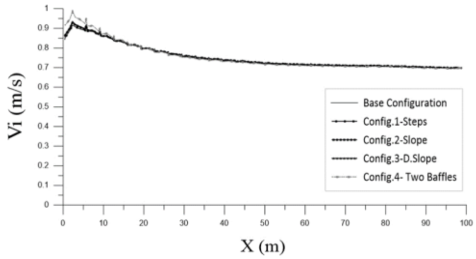

Fig. 16: Velocity distribution for all configurations compared to initial configuration at cross section 3.

7.3 Influence of intake angle on flow uniformity

The analyzing of the circulation zone area, length, and width for configuration 4 at angles 60°, 45°, and 30° was examined in contrast to a right intake angle as demonstrated from Figure 17 to Figure 20. Results showed significant reductions in these parameters. For angle 60°, the decrease was approximately 68%, 46%, and 41% in case of circulation zone area, length, and width, respectively. For angle 45°, the reductions were about 76%, 58%, and 47% respectively, while for angle 30°, the reductions were about 91%, 57%, and 53% respectively.

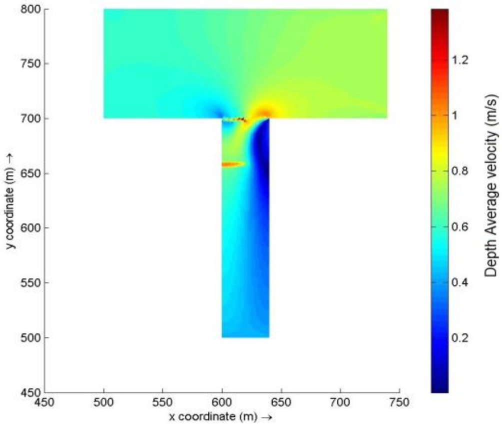

Fig. 17: Color scheme of 2D current plot for configuration 4 at angle 90°.

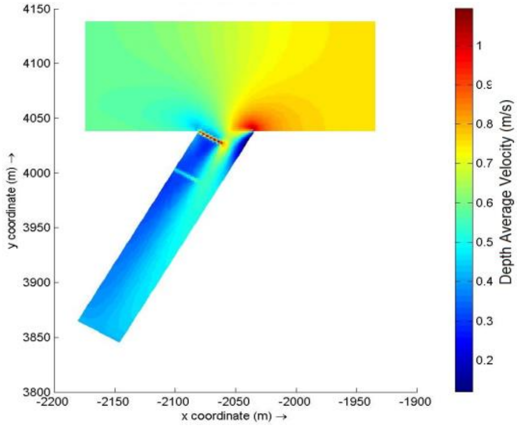

Fig. 18: Color scheme of 2D current plot for configuration 4 at angle 60°.

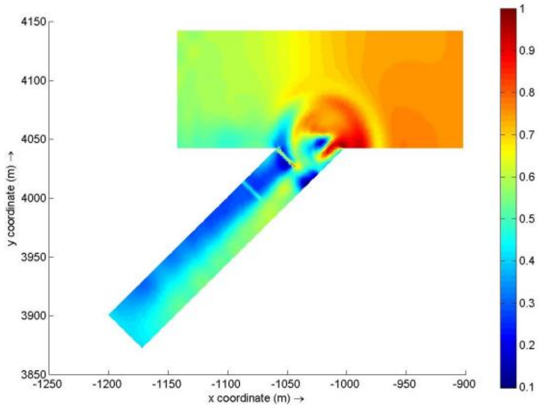

Fig. 19: Color scheme of 2D current plot for configuration 4 at angle 45°

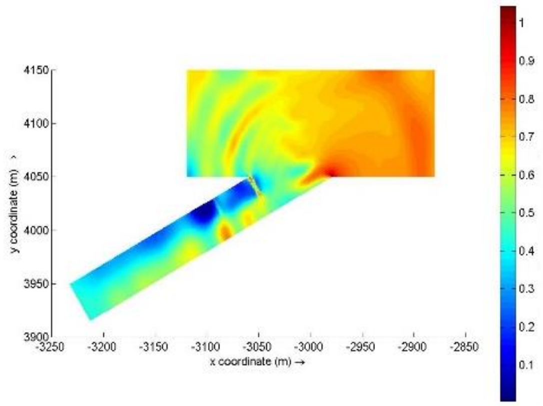

Fig. 20: Color scheme of 2D current plot for configuration 4 at angle 30°

Furthermore, the velocity distribution across the intake channel was plotted and compared for configuration 4 at angles 90°, 60°, 45°, and 30°. A noticeable reduction in high velocities at the right side was observed at cross section 5 for angle 60° (49% reduction), angle 45° (51% reduction), and angle 30° (62% reduction) if compared to the reference angle of 90°, as depicted in Figure 21. Generically, the intake orientations at angles 60°, 45°, and 30° led to an improvement in velocity distribution at sections 5, 6, and 7. Particularly, the reverse flow that occurred at the left side in case of configuration 4, which remained unresolved in other configurations, was significantly reduced, and resulting in improving the shape of velocity distribution at section 5.

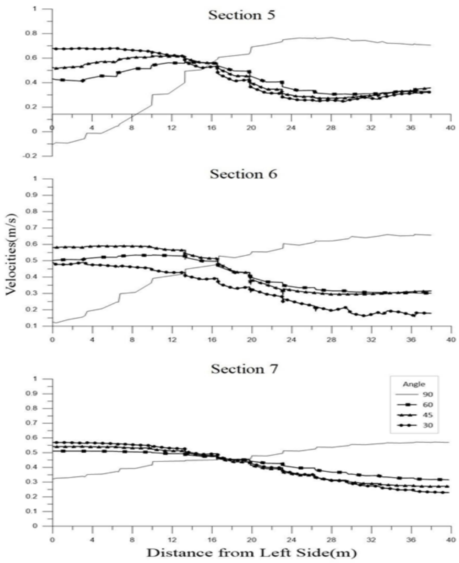

Fig. 21: Velocity distribution for different angles at section 5, 6, and 7 for Configuration 4.

For more scrutiny, both relative vortex width (Wv/Wch) and length (Lv/Lch) were studied against the changing of θ. This was carried out for configuration 4 and 1, as shown in Figure 22. For Configuration 4, it was noticed that there were significant improvements which achieved at angle 30° compared to angle 90°, i.e., Lv/Lch decreased from 24% (θ = 90°) to 9% (θ = 30°), likewise, Wv/Wch reduced from 23% (θ = 90°) to 10% (θ = 30°). This describes that angle 30 has a great effect in decreasing the vortex dimensions. For configuration 1, it was tested to confirm that the angle effect had the same trend over different configurations. It was observed also that there was a reduction of 45% and 60% in vortex length and width ratios, respectively.

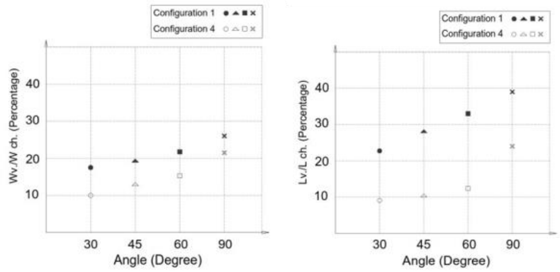

Fig. 22: (left) The intake angle (θ) versus the relative vortex width (Wv/Wch). (right) The intake angle θ versus the relative vortex length (Lv/Lch).

8. Conclusions

The influence of geometric design attributes on the flow separations developed at open channel intake entrance was examined. The study is an attempt to maximize the efficiency of water withdrawal by minimizing the intake vortices and improving flow consistency. Sensitivity of design attributes including intake bed geometry (slope and steps), and angles were examined for improving flow circulation zone by using Delft3D-FM numerical model.

Velocity distribution inside the intake was improved in all configurations compared to base configuration or initial configuration. Configuration 4 improved flow velocity by 25%, configuration 3 by about 9.3%, configuration 2 by about 17.3%, and configuration 1 by about 11%.

Circulation zones were improved in all configurations compared to base case. Configuration 4 reduced circulation zone by 40%, configuration 3 by about 36.36%, Configuration 2 by about 11.36%, and configuration 1 by about 5.45%.

Reverse flow width was improved in all configurations compared to initial configuration also. Configuration 4 reduced circulation zone by 21.25%, configuration 3 by about 17.5%, Configuration 2 by about 24%, and configuration 1 by about 26%.

In addition, velocities distributions were tested for all configurations in the main channel in front of the intake. This comparison showed that there was a slight increase in velocity in the case of configuration 4 compared with other configurations. This difference didn't exceed 3 % and 5 % at upstream and downstream corners of the intake.

Moreover, Configuration 4 was tested for three intake angles. The intake angle has a significant effect on the flow circulation and consistency inside the intake. Intake oriented at angle 60° decreased circulation zone by 68% compared to right angle intake and intake oriented at angle 30° decreased circulation zone by 91%.

Generally, these design attributes showed a significant effect that were studied intensively in this study. Configuration 1, 2 and 3 showed little effect on improving flow consistency inside the intake. However, configuration 4 showed a significant effect on enforcing the flow to the inner side and achieving a good flow distribution inside the intake. In terms of intake angle, the minimum the intake angle that was measured from the downstream direction, the minimum the flow circulation was observed. The findings presented herein can provide insights for decision makers and designers during conceptual design for the intake geometry selection process.

References

[1] Raudkivi, "Sedimentation: exclusion and removal of sediment from diverted water", Auckland, New Zealand, CRC Press, 1st edition, 1993.

[2] Hamid Sh. and Bahareh P., "Investigation of characteristics of separation zones in T- junctions", WSEAS transactions on mathematics, Vol. 5, No. 7, pp. 303-312, 2008.

[3] Yonesi H., Omid H., and Haghiabi H., "A study of the effects of the longitudinal arrangement sediment behavior near intake structures", J. Hydraul. Res., Vol. 46, No. 6, pp. 814-819, 2008.

[4] Sayed T., "An experimental study of branching flow in open channels", Limnological Review, Vol. 19, No. 2, pp. 93-101, 2019.

[5] Barkdoll B., Ettema R., and Odgaard A., "Sediment control at lateral diversions: Limits and enhancements to vane use", Journal of Hydraulic Engineering, Vol. 125, No. 8, pp. 862-870, 1999.

[6] Shamloo H. and Pirzadeh B., "Numerical investigation of velocity field in dividing open channel flow", Proceedings of the 12th WSEAS International Conference on APPLIED MATHEMATICS, Cairo, Egypt, December 29-31, pp. 194-198, 2007.

[7] Jalili H., Hosseinzadeh A., and Farsadizadeh D., "Effect of intake geometry on the sediment transport and flow pattern at lateral intake", Iranian Water Research Journal, Vol. 5, No. 9, pp. 1-10, 2011.

[8] Neary v., Sotiropoulous F., and Odgaard J., "Three-dimensional numerical model of lateral-intake inflows", Journal of hydraulic engineering, Vol. 125, No. 2, pp. 126-140, 1999.

[9] Ramamurthy A., Junying Q., and Diep v., "Numerical and experimental study of dividing open-channel flows. Journal of hydraulic engineering", Vol. 133, No. 10, pp. 1135-1144, 2007.

[10] Rady M. A., "2-D Modelling of the Impact of Changing Hydraulic Parameters on the Flow Pattern at Right-angled Open Channel Confluences", Nile Water Science & Engineering Journal, Vol. 8, No. 2, pp. 1–13, 2015.

[11] Nikbin S. and Borghei S., "Experimental investigation of submerged vanes effect on dimensions of flow separation zone at 90° open channel junction", 6rd National Congress on Civil Engineering, University of Semnan, (In Persian), 2011.

[12] Goudarzizadeh R., Hedayat N., and Jahromi S. M., "Three-dimensional simulation of flow pattern at the lateral intake in straight path, using finite-volume method", World Academy of Science, Engineering and Technology, Vol. 47, pp. 656-661, 2010.

[13] Seyedian S., Karami K., and Shafai M., "Determine the optimal radius in lateral intakes 55° and 90° using variation of flow velocity", 2008.

[14] Keshavarzi A., and Habibi L., "Optimizing water intake angle by flow separation analysis", Irrigation and Drainage, Vol. 54, No. 5, pp. 543–552, 2005.

[15] Karami M. and Keshavarzi E., "Investigation on flow pattern in the intakes of 56 and 90 degree with edged entrance", 3rd national congress on civil engineering, 1-3 May, University of Tabriz, Tabriz, Iran, 2007.

[16] Ouyang H.T., "Investigation on the dimensions and shape of a submerged vane for sediment management in alluvial channels", Journal of hydraulic engineering, Vol. 135, No. 3, pp. 209-217, 2009.

[17] Rooniyan F., "The Effect of Confluence Angle on the Flow Pattern at a Rectangular Open Channel", Engineering Technology & Applied Science Research, Vol. 4, No. 1, pp. 576-580, 2014.

[18] Al-Zubaidy R. and Hilo A., "Numerical investigation of flow behaviour at the lateral intake using Computational Fluid Dynamics (CFD)", Water Supply, Vol. 22, No. 4, pp. 4193-4206, 2021.

[19] Al Omari N. K. and Khaleel M. S., "Laboratory study of the effect of the branching angle and the branching channel slope on flow", Al-Rafadain Engineering Journal, Vol.2 0, No. 5, pp. 33-41, 2012.

[20] Roelvink J. A. and Van Banning G. K. F. M., "Design and development of DELFT3D and application to coastal morphodynamic", Oceanographic Literature Review, Vol. 11, No. 42, pp. 925, 1995.

[21] Hu K., Ding P., and Yang S., "A 2d/3d hydrodynamic and sediment transport model for the Yangtze estuary", journal of marine systems, Vol. 77, pp. 114-136, 2009.

[22] Lesser G., "development and validation of a three-dimensional morphological model", Coastal engineering, Vol. 51, No. 89, pp. 883-915, 2004.

[23] Ammar A. A. and Sven K., "Three-Dimensional Morphodynamical Modelling of Tigris River in Baghdad", Journal of Civil Engineering and Architecture, Vol. 11, No.1, pp. 571-594, 2017.